

## Conference paper

Maria Diletta Pianorsi, Martina Raudino, Nicole Bonelli, David Chelazzi, Rodorico Giorgi, Emiliano Fratini and Piero Baglioni\*

# Organogels for the cleaning of artifacts

DOI 10.1515/pac-2016-0908

**Abstract:** The cleaning of artifacts must not alter the original properties of the objects. While the use of free solvents is risky, their confinement into polymeric networks can allow the safe removal of unwanted layers from artifacts. Recently, a methyl 2-methylprop-2-enoate (MMA)-based organogel was formulated as loaded with butan-2-one (MEK), and used to remove aged varnishes from canvas paintings. However, this formulation is not enough retentive to allow its use on paper, where higher retentiveness is needed to avoid the uncontrolled spreading of MEK and dissolved materials. Here, a new PMMA-MEK gel was designed to overcome this limitation. The amount of cross-linker and monomer used in the synthesis of the gel were tuned to achieve optimal retentiveness. Differential scanning calorimetry (DSC), differential thermogravimetry (DTG), small-angle X-ray scattering (SAXS) and attenuated total reflection fourier transform infrared spectroscopy (ATR-FTIR) provided information on the solvent content, release rate, and mesoporosity of the gel as compared to the previous system. The lower solvent release rate of the new formulation allowed the safe removal of wax that jeopardized a 19<sup>th</sup> century paper document. The removal was confirmed through optical microscopy and ATR-FTIR, which also highlighted the absence of gel residues on the treated surface.

**Keywords:** cleaning; colloids; methyl methacrylate; organogels; paper artworks; POC-16.


## Introduction

Cleaning is one of the most controversial procedures in the field of conservation of works of art. The non-reversibility of the treatment requires high selectivity in the cleaning intervention and no risks for the original materials, especially in the case of solvent- or water-sensitive works of art like paper sheets, manuscripts, books and other documents. In fact, historical collections and archives are typically contaminated by deposits of soiling and detrimental materials, such as aged adhesives or natural polymeric coatings used in past restoration interventions, which alter the appearance and readability of the artifacts. Besides, aged coatings can develop acidic compounds that promote the acid hydrolysis of cellulose, a degradation process already favored by the presence of several compounds (e.g. lignin) coming from the paper making process [1]. Usually, all the undesired materials to be removed from these artifacts are confined in a surface layer (roughly 20–200  $\mu\text{m}$  thick) characterized by the co-presence of art media (e.g. pastel, pencil, charcoal or ink), which are not firmly bound to the substrate. This makes the cleaning and preservation of cellulosic-based artworks a challenging task for conservators worldwide.

**Article note:** A collection of invited papers based on presentations at the 16<sup>th</sup> International Conference on Polymers and Organics Chemistry (POC-16), Hersonissos (near Heraklion), Crete, Greece, 13–16 June 2016.

**\*Corresponding author: Piero Baglioni**, Department of Chemistry Ugo Schiff and CSGI, University of Florence, Via della Lastruccia 3, Sesto Fiorentino, 50019 Florence, Italy, e-mail: baglioni@csgi.unifi.it

**Maria Diletta Pianorsi, Martina Raudino, Nicole Bonelli, David Chelazzi, Rodorico Giorgi and Emiliano Fratini:** Department of Chemistry Ugo Schiff and CSGI, University of Florence, Via della Lastruccia 3, Sesto Fiorentino, 50019 Florence, Italy

 © 2017 IUPAC & De Gruyter. This work is licensed under a Creative Commons Attribution-NonCommercial-NoDerivatives 4.0 International License. For more information, please visit: <http://creativecommons.org/licenses/by-nc-nd/4.0/>

Brought to you by | Università degli Studi di Firenze  
Authenticated

Download Date | 3/22/17 11:18 AM

Traditional cleaning methods, e.g. dry mechanical action or removal by mixtures of organic solvents [2], involve several drawbacks, especially when the treatment is carried out on naturally aged and degraded objects such as fragile aged paper. Dry cleaning can be potentially aggressive, uncontrolled and unselective, especially when it is carried out with traditional tools, i.e. brush, cotton swab and scalpel. Wet cleaning with free organic solvents may cause the uncontrolled penetration of the fluids through the paper fibers network, and consequently the solubilization of solvent-sensitive original materials (inks, pigments, dyes). Moreover, any solubilized detrimental material (e.g. soiling) can be re-transported by the solvent through the cellulosic substrate, making its effective removal even more difficult [3]. Additionally, the high volatility and toxicity of organic solvents commonly used in the restoration practice, limit their application owing to the potentially harmful effects on both the operators and the environment.

In order to overcome these issues, gel systems have been developed for the preservation of artifacts, where cleaning liquids are confined into polymeric matrices. This allows the controlled release of the fluids onto water- or solvent-sensitive surfaces and reduces the volatility of the confined solvents. Chemical hydrogels made of semi-interpenetrating (SIPN) poly(2-hydroxyethyl methacrylate) (pHEMA) and 1-ethenylpyrrolidin-2-one (PVP) have already been used for the cleaning of canvas paintings surfaces [3–6], and were recently loaded with an aqueous oil-in-water (o/w) nanostructured fluid for the cleaning of collagen-based artifacts [7]. These gels were designed to exhibit optimal properties in terms of mechanical behavior and retentiveness, which allows their application and removal without leaving detectable residues (as verified by FTIR spectroscopy) [3–7].

Chemical “organogels” (i.e. where the confined fluids are organic solvents rather than aqueous systems) can be used as cleaning tools complementary to hydrogels, maintaining good retentiveness and mechanical properties. The confinement of organic solvents, with lower polarity than water, broadens the applicability of gels for the removal of coatings found on the surface of artifacts. In a previous work, a methyl 2-methylprop-2-enoate (MMA)-based organogel was prepared as loaded with butan-2-one (MEK), and applied on painted canvas samples for the safe removal of polymeric surface coatings [8]. This formulation worked well on painted canvas, however it is not enough retentive to allow safe application on paper substrates that are more sensitive to solvents as compared to varnished canvas paintings, owing to different surface properties (i.e. higher porosity and different chemical affinity to solvents). Therefore, in the present work we decided to improve on this formulation by developing a new PMMA-MEK organogel, specifically designed for the selective removal of wax contaminants from the surface of ancient inked paper. This case study was selected because of its representativeness in the real conservation practice, where the selective removal of wax residues is a typical and challenging issue faced by paper conservators. The retentiveness of the new gel network was specifically increased by systematically tuning the amount of cross-linker (which was increased) and the monomer-solvent phase ratio during the synthesis of the gel, which was carried out through the free radical polymerization of MMA in pure MEK. The latter was selected because it is a versatile solvent capable of dissolving or swelling numerous natural and synthetic coatings; in fact, preliminary tests carried out in the framework of the present work showed that the solvent was able to soften and swell the wax contaminant found on the paper document that was selected for the cleaning intervention.

We report here the physico-chemical characterization of the new poly(methyl 2-methylpropenoate) (PMMA) organogel formulations, as compared to that of the previous PMMA-MEK formulation. The presence of unreacted monomer in the polymer network was assessed with attenuated total reflection Fourier transform infrared spectroscopy (ATR-FTIR). Small-angle X-ray scattering (SAXS) was used to detail the mesoporosity and the nanoscale structure of the gel systems. Calorimetric analysis was employed to obtain information on the affinity of the PMMA network to the liquid phase. In particular, thermogravimetric analysis (TGA) was used to check the equilibrium solvent content of the gels, while differential scanning calorimetry (DSC) was employed to determine their glass transition temperature. The solvent evaporation and release rate of the gels (gravimetrically measured) were compared. Finally, the chemical organogels were applied on a real sample of ancient inked paper, for the removal of wax spots. The chemical composition of the wax was assessed with ATR-FTIR, before carrying out the removal of the spots with the gels. The release control of the new gel on paper was compared to that of the previous formulation. After the intervention,

the absence of gel residues and the efficiency of the treatment were confirmed by optical microscopy (OM) and ATR-FTIR analysis.

## Experimental details

### Chemicals

Methyl 2-methylprop-2-enoate (MMA) (Sigma-Aldrich, purity  $\geq 99\%$ ), 2-(2-Methyl-acryloyloxy)ethyl 2-methyl-acrylate (EGDMA) (Sigma-Aldrich, purity  $\geq 99\%$ ), 2,2'-Azobis(2-methylpropionitrile) (AIBN) (Fluka, purity  $> 98\%$ ), and butan-2-one (MEK) (Sigma-Aldrich purity  $\geq 99\%$ ) were used for the syntheses of the gels. All chemicals were used as received.

### Gel preparation

In order to obtain gels harder and more retentive than those prepared in a previous work [8], the percentage of cross-linker was increased, up to values ranging from 1 to 3% (w/w) of the total MMA quantity. The new gels have been labeled as PMMA-MEK.1–3, where PMMA-MEK.1 has the lowest amount of EGDMA, and PMMA-MEK.3 has the highest. The quantity of MMA monomer with respect to MEK was adjusted to 30% (w/w). The PMMA organogels were obtained by free radical copolymerization of MMA and EGDMA (cross-linker) in solution. MMA was solubilized in pure MEK, and AIBN (1.64% w/w as compared to MMA) was added to initiate the radical reaction.

The synthesis was carried out in two types of molds to obtain organogels with different final shapes: cylinders ( $2.5 \times 2.5 \times 1 \text{ cm}^3$ ) were used to carry out the gel characterization, while flat organogel sheets (2 mm thick) were deemed optimal for the cleaning tests. The molds were PTFE cylinders with an inner diameter of 2.5 cm resistant to chemicals and high temperatures, and a glass caster. Three gels were synthesized of each type. The containers were sealed and placed into an oven, following the procedure reported elsewhere [8]. In order to remove any unreacted monomer, the gels were then washed by immersion into plastic vials (30 mL) filled with MEK. The washing solvent was discarded and renewed daily. After seven washing cycles, the organogels were finally equilibrated with MEK through immersion in the solvent, before use.

### Gel characterization

#### Reaction yield and monomer residues

The reaction yield was then calculated as follows:

$$\text{yield(\%)} = \frac{\text{amount of obtained polymer}}{\text{amount of monomer}} \times 100 \quad (1)$$

The 'amount of monomers' is the weight in grams used for the preparation of the gel and the 'amount of obtained polymer' after the reaction is calculated by weighing the oven-dried gel. Before drying, the gels were washed several times, to remove all the unreacted monomers.

Information about the presence of unreacted monomer contained inside the gels, was collected using ATR-FTIR: after each washing cycle (see above), the gels were soaked in 5 mL of MEK overnight, to allow the molecules of monomer still present to migrate in the surrounding solvent; then ATR measures were made on this liquid, called 'Exchange solvent', to verify the presence of unreacted monomer. Measurements were carried out daily for 7 days. A Thermo Nicolet Nexus 870 FTIR spectrometer equipped with a Golden Gate diamond ATR with 128 scans and  $4 \text{ cm}^{-1}$  of optical resolution, in the  $4000\text{--}450 \text{ cm}^{-1}$  range, was used.

### Equilibrium solvent content ( $Q$ )

The equilibrium solvent content ( $Q$ ) values were obtained as follows:

$$Q(\%) = \frac{W_i - W_d}{W_d} \times 100 \quad (2)$$

where  $W_i$  is the weight of the completely swollen gel, and  $W_d$  is the weight of the dry sample.

The weight of the wet samples,  $W_i$ , was determined at two different times: 1) after preparation and 7 days of immersion in MEK; 2) on gels that were completely dry after preparation, and then let equilibrate with the solvent. This second measurement was carried out to verify if possible alterations of the porous structure (e.g. pore collapse), occurred during the drying, affect the equilibrium solvent content. Accordingly, two different values of  $Q$  were obtained, the first being defined as  $Q_1$  (before drying) and the second as  $Q_2$  (after re-loading with the solvent).

The equilibrium solvent content before drying ( $Q_1$ ) was also checked via Differential Thermogravimetry (DTG). The instrument used was a SDT Q600 (TA INSTRUMENTS). Measurements were performed in a nitrogen atmosphere with a sample purge flow rate of 100 mL/min. The temperature scan used in the experimental procedure was from 20 to 500 °C, at constant heating rate of 10 °C/min.

### Solvent release kinetics

In order to study the release kinetic of MEK, we investigated the decrease of the evaporation rate of MEK when confined in the PMMA-MEK gels. Both free and confined MEK were exposed at room temperature (25 °C) and RH 60 %. The loss of weight of swollen PMMA-MEK gels was compared to that of petri dishes containing the same mass of free MEK. Only normal air circulation was used (no ventilation/aspiration). To assess the rate of solvent release of the new PMMA-MEK formulations on porous substrates that mimic paper artifacts, the gels were placed on a Whatman® sheet (diameter 55 mm), and covered with a foil of Mylar® to prevent evaporation of the solvent. The quantity of released solvent was measured by weighing the Whatman® sheet over time, and then the residual solvent content of the gels was calculated accordingly.

### SAXS measurements

Small-angle X-ray scattering (SAXS) measurements were performed using a HECUS S3-Micro (Kratky-type camera) equipped with a position-sensitive detector (OED 50 M) containing 1024 channels of width 54 μm. Cu Kα radiation of wavelength  $\lambda = 1.542 \text{ \AA}$  was provided by a GeniX X-ray generator (Xenocs, Grenoble) working with a microfocus sealed-tube operating at a power of 50 W. The volume between the sample and the detector was kept under vacuum during the measurements to minimize scattering from the air. Scattering curves were obtained in the  $q$ -range between 0.01 and  $0.55 \text{ \AA}^{-1}$ . Gel samples were placed into a 1 mm demountable cell with Kapton films as windows. The temperature was set to 25 °C and was controlled by a Peltier element, with an accuracy of  $\pm 0.1 \text{ °C}$ . Scattering curves were corrected for the empty cell contribution and for the scattering of the Kapton films, considering the relative transmission factors.

### Differential scanning calorimetry (DSC)

Differential scanning calorimetry (DSC) was carried out to evaluate the glass-transition temperature ( $T_g$ ) of the PMMA-MEK gels, using a Q2000 Calorimeter (TA INSTRUMENTS). Measures were carried out at a con-

stant nitrogen flow rate of 50 mL/min. Experiments were performed in the temperature range from 25 to 180 °C, with a constant heating rate of 10 °C/min. Samples of gels (5–6 mg) were put into a Tzero® standard aluminum pan.

## Results and discussion

### Characterization of the PMMA-MEK organogels

#### Reaction yield and monomer residues

The synthesis reaction yield was 85.4 %, 82.9 % and 85.6 % for, respectively, PMMA-MEK.1–3. The yield values are similar or slightly higher than that obtained in the previous work (ca. 83 %), where lower amounts of cross-linkers were used [8]. However, because the yield was not complete, the presence of monomer residues was investigated using ATR-FTIR. Measures were carried out on the ‘Exchange solvent’, as specified in Section “Gel characterization”, in order to verify the presence of any unreacted monomer. Measurements were carried out daily for 7 days. Figure 1 shows the comparison between the ATR-FTIR spectra of MMA, MEK, and the exchange solvent. The spectra of MEK and of the exchange solvent (both after 2 and 7 cycles) were normalized at 1716  $\text{cm}^{-1}$  (C=O str. of MEK), while the spectrum of MMA was kept at a different scale to help the readability of the graphs. Already after two washing cycles, most of the unreacted monomer is removed, similarly to what was found in the previous work [8]. Overall, seven washing cycles were necessary to obtain a gel free of monomer, as shown by the disappearance of the MMA bands at 815 ( $\nu_s$  C–O–C) and 820  $\text{cm}^{-1}$  ( $\text{CH}_2$  rock), which were highlighted as they do not overlap with any band of MEK.

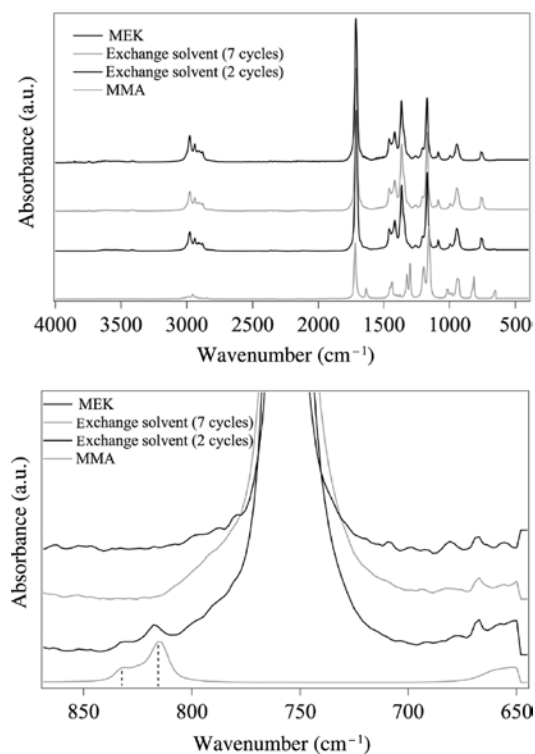


**Fig. 1:** ATR-FTIR spectra of MEK that was let to exchange with a PMMA-MEK organogel after two and seven washing cycles, as compared to the spectra of MEK, and MMA. The bottom panel shows a detail of the 850–650  $\text{cm}^{-1}$  region.

## Equilibrium solvent content ( $Q$ )

Table 1 lists the values of the equilibrium solvent content ( $Q$ ) of the organogels that were equilibrated 7 days with MEK right after the synthesis ( $Q_1$ ), and for the gels dried after the synthesis and then re-loaded with MEK ( $Q_2$ ). For all the PMMA-MEK formulations, the equilibrium solvent content is higher than the percentage of MEK used during the synthesis (“Preparation MEK” in Table 1), which confirms that MEK has a high affinity for the PMMA polymeric network. Overall, both  $Q_1$  and  $Q_2$  of the new gels are lower than that of the PMMA-MEK previously developed [8], which is in agreement with the highest amount of cross-linker used in the new formulations. In principle, in the case of dried and re-solvated gels a partial collapse of the porous structure could be expected during the drying process, leading to lower values of  $Q_2$  as compared to  $Q_1$ . However, in the case of PMMA-MEK.1–3, the difference between  $Q_1$  and  $Q_2$  is almost irrelevant. The  $Q_1$  values obtained through DTG for the PMMA-MEK.1–3 formulations are, respectively, 83.2%, 85.7%, and 84.7%, in good agreement with the values obtained gravimetrically.

## Solvent release kinetics

We studied the evaporation rate of MEK when confined in the PMMA-MEK gels. We investigated both the PMMA-MEK.3 formulation, and the PMMA-MEK gel developed previously [8]. Figure 2 (top panel) shows the evaporation of MEK in the two organogels, and that of the non-confined solvent.

Similarly to a drying process, the evaporation of a solvent from a porous substrate (i.e. the gel matrix) involves both heat and mass transfer through the polymeric network. To evaporate, the liquid must travel through the network, and once it reaches the boundary it is transported away by the surrounding gas (in our case, air). The experimental curves for the PMMA-MEK and PMMA-MEK.3 formulations (see Fig. 2) do not show any period where the drying rate is constant, instead the drying rate falls continuously in time. In these conditions (falling rate drying period) the internal heat and mass transfer rates determine the rate at which the solvent becomes available at the exposed evaporating surface [9]. In this case, since the drying takes place at temperatures below the boiling point of the solvent, diffusional mass transfer is the most commonly assumed mechanism of transfer of the liquid phase [9]. Diffusion in polymeric networks was extensively studied in the field of controlled drug release. Peppas and Korsmeyer [10] proposed a simple, semi-empirical equation to describe release through diffusion within a polymeric matrix:

$$M_t / M_\infty = kt^n \quad (3)$$

where  $M_t$  and  $M_\infty$  are, respectively, the absolute cumulative amount of solvent released at time  $t$ , and at infinite time (which corresponds in our system to the initial amount of solvent contained in the system, i.e. the  $Q_1$  values listed in Table 1),  $k$  is a constant related to the structural and geometric characteristics, and  $n$  a parameter related to the diffusion mechanism. This model takes into account both Fickian and non-Fickian (case-II and anomalous transport) diffusion, which are two independent mechanisms that may superpose in case of mass transport within polymer networks. The value of the release exponent  $n$  ranges between 0.5 (completely diffusion-controlled release, i.e. Fickian diffusion) and 1 (completely swelling-controlled release,

**Table 1:** Equilibrium solvent content (measured gravimetrically) of PMMA-MEK organogels after preparation and 7 days of solvent immersion ( $Q_1$ ), and of gels that were completely dry after preparation, and then re-loaded with MEK ( $Q_2$ ).

Sample	Preparation MEK (% w/w)	$Q_1$ ( $\pm 0.1$ %)	$Q_2$ ( $\pm 0.1$ %)
PMMA-MEK.1	70.0	82.4	82.3
PMMA-MEK.2	70.0	84.7	84.6
PMMA-MEK.3	70.0	84.4	84.3
PMMA-MEK previously developed (see Ref. [8])	59.5	91.1	90.6

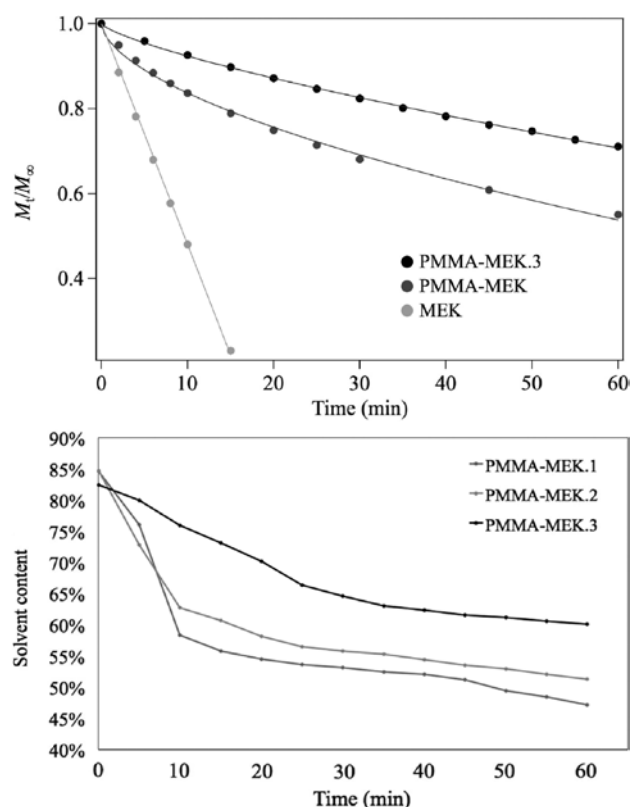


**Fig. 2:** (Top) Solvent fraction released through evaporation of free MEK (from petri dishes) as compared to that of MEK confined in the PMMA-MEK.3 formulation, and in a PMMA-MEK gel previously developed using lower quantity of cross-linker [8]. Circles represent experimental data, solid lines represent best fittings according to a zero-order kinetics (free MEK), or to the Peppas-Korsmeyer model [10] (PMMA-MEK, PMMA-MEK.3). (Bottom) Solvent release kinetic curves of the PMMA-MEK.1–3 organogels, expressed as solvent content of the gels during the first hour of application on a model paper substrate.

i.e. case-II transport). All transport processes with intermediate  $n$  values can be regarded as a superposition of both phenomena (the so-called anomalous transport). It must be noticed that the diffusivity is also a function of temperature, thus the liquid diffusion model should be regarded purely as an empirical representation in the falling rate drying period [9].

Figure 2 shows that the non-confined solvent follows a zero-order kinetics (constant evaporation rate), where solvent is released at constant rate until its complete evaporation after 15 min. On the other hand, the evaporation rates of the solvent confined into the organogel formulations are much lower. In fact, after 60 min, the PMMA-MEK and PMMA-MEK.3 formulations contain, respectively a solvent fraction of 0.55 and 0.77 as compared to their initial solvent content. Fitting of the curves with the Peppas-Korsmeyer model yields values of the release exponent  $n$  that indicate an anomalous transport mechanism for both the formulations. PMMA-MEK exhibits a lower release exponent ( $n=0.58$ ) denoting that the process is predominantly diffusion controlled, while the higher  $n$  value ( $n=0.75$ ) of PMMA-MEK.3 indicates that in this case polymer relaxation is the step that governs mass transfer within the polymer matrix. This result is consistent with the higher amount of cross-linker used for PMMA-MEK.3, and with the lower  $Q$  value of this formulation, as compared to PMMA-MEK. Higher amounts of cross-linker result in lower pore size, and increased rigidity of the polymer network, which hamper the solvent transport by simple diffusion mechanism, resulting in lower release rates and lower fraction of released solvent after 60 min.

Figure 2 (bottom panel) shows the rate of solvent release of the new PMMA-MEK formulations on porous substrates that mimic paper artifacts. The solvent content values at  $t=0$  correspond to the percentage of liquid phase after 7 days of swelling the gels with MEK, i.e. the  $Q_1$  values listed in Table 1. Consistently with the evaporation kinetics discussed above, also in this case the PMMA-MEK.3 gel exhibits a slower and more

gradual release than PMMA-MEK.1–2, especially during the first 25 min (representative of typical application times of gels in cleaning interventions). The slower release kinetic of PMMA-MEK.3, hence its higher retentiveness as compared to the other two formulations, is consistent with the higher percentage of cross-linker used than for PMMA-MEK.1–2.

Based on the obtained results, the PMMA-MEK.3 formulation was selected as the optimal system for application on inked paper surfaces. In fact, both the lower evaporation rate and the more gradual release on porous substrates are features with important applicative relevance, as they allow decreasing the impact of solvents on operators during the cleaning intervention, and reducing solvent spreading and penetration on the treated paper artifact. Moreover, the PMMA-MEK.3 gel also exhibits optimal optical transparency and mechanical properties in terms of easiness of handling (see Fig. 3).

### SAXS measurements

The relatively low volatility of MEK made it difficult to obtain xerogels through lyophilization without significantly affecting the pore structure; therefore, the investigation of the PMMA-MEK organogels through scanning electron microscopy did not provide exhaustive information on their porosity. Thus, SAXS measurement was performed to detail the nano-scale structure and the mesoporosity of the swollen organogel. The scattering curve was interpreted using the Debye-Bueche model [11]:

$$I(q) = I_{\text{Lor}}(q) + I_{\text{ex}}(q) + bkg \quad (4)$$

where

$$I_{\text{Lor}}(q) = \frac{I_{\text{Lor}}(0)}{1 + q^2 \xi^2} \quad (5)$$

$I_{\text{Lor}}(0)$  is the scattering intensity at  $q=0$ , dependent from the contrast between the polymer and the solvent and from the volume fraction of the polymer in the gel, and  $\xi$  is the characteristic mesh size of the network.

$$I_{\text{ex}}(q) = \frac{I_{\text{ex}}(0)}{(1 + q^2 a^2)^2} \quad (6)$$

$I_{\text{ex}}(0)$  represents the excess intensity at  $q=0$  and  $a$  is the size of gel inhomogeneities.

The SAXS curve of the PMMA-MEK.3 gel is shown in Fig. 4 and the results of the Debye-Bueche fitting are listed in Table 2, as compared to those of the PMMA-MEK previously developed for the cleaning of canvas paintings.

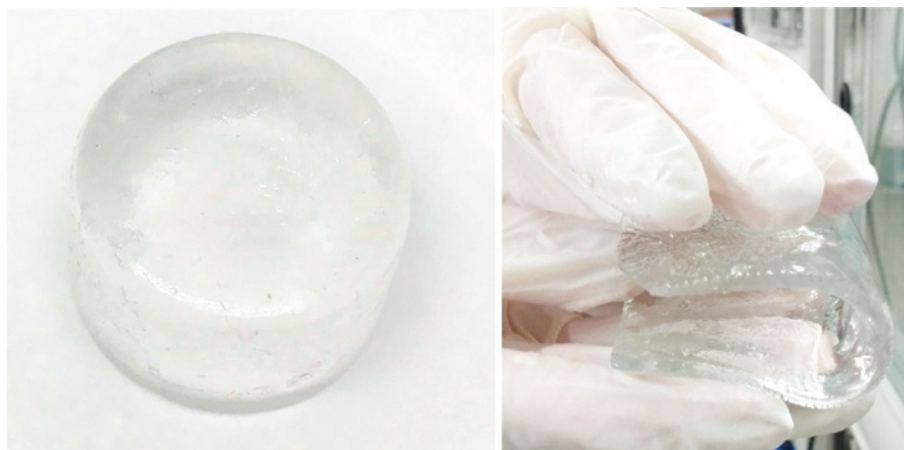


Fig. 3: PMMA-MEK.3 organogels. (Left) cylinder-like shape. (Right) Flat sheet.



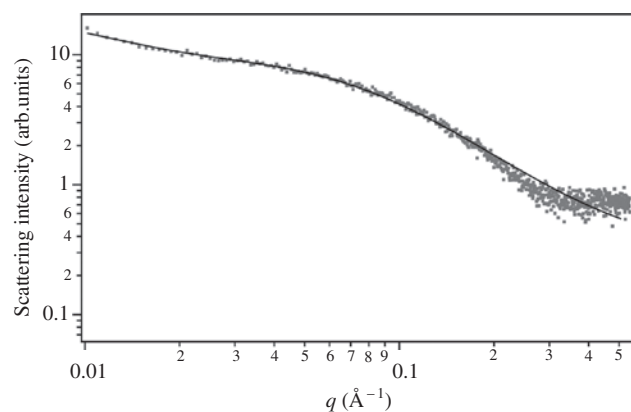


Fig. 4: SAXS curve (dots) and Debye-Bueche fit (solid line) of the PMMA-MEK.3 organogel.

Table 2: SAXS fitting parameters of the PMMA-MEK.3 organogel as compared to those of the PMMA-MEK previously developed for the cleaning of canvas paintings.

Fitting parameters	PMMA-MEK.3	PMMA-MEK previously developed (see Ref. [8])
$I_{\text{Lor}}(0)$	$9.55 \pm 0.08$	$47.1 \pm 0.3$
$\xi$ (nm)	$1.21 \pm 0.01$	$1.59 \pm 0.01$
$I_{\text{exc}}(0)$	$12.00 \pm 1.15$	$18.1 \pm 0.5$
$a$ (nm)	$7.3 \pm 0.4$	$5.5 \pm 0.2$
$bkg$	$0.30 \pm 0.01$	$0.40 \pm 0.05$

The new gel shows a slightly lower mesh size as compared to that of the PMMA-MEK formulation reported in previous work [8]. This result can be explained considering that the PMMA-MEK.3 gel has a lower equilibrium solvent content, which is known to affect  $\xi$  [12]. The lower mesh size of PMMA-MEK.3 is consistent with the slower solvent release rate of this formulation as compared to PMMA-MEK, as highlighted in the previous section, because the lower mesh size is expected to hinder the transport of solvent through the polymer network.

The size of gel inhomogeneities ( $a$ ) is slightly higher for the PMMA-MEK.3 formulation as compared to its predecessor. It must be noticed that a high concentration of cross-links in the gel network leads to greatly disordered structures (solid-like regions) [13–15]. Overall, the increased amount of cross-linker used in the synthesis of the new gel led to a decrease in the mesoporosity, which could contribute to its higher retentiveness, a feature required for applications on paper.

### Differential scanning calorimetry (DSC)

The glass transition temperature ( $T_g$ ) of the PMMA-MEK gels was determined through DSC. The literature reports different values for the  $T_g$  of PMMA [16, 17], depending on the degree of tacticity, thermal history, type of filler, morphology, inter-crystallite distance, and the type of free radical initiator used during processing [18–22]. The DSC measurements carried out in the present work indicated that there is no significant change in the heat flow behavior between pure PMMA and the PMMA-MEK systems. In the case of PMMA-MEK.3 sample, we obtained an experimental value of  $95.2^\circ\text{C}$  (see Fig. 5), which falls in the  $T_g$  range of “commercial grade” PMMA ( $85\text{--}165^\circ\text{C}$ ) [23], such as that used for the synthesis of the organogel. The low values of heat flow recorded suggest that the network is highly disordered, in agreement with the SAXS results.

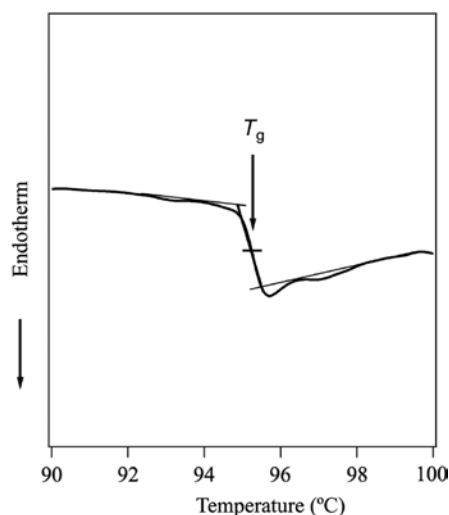


Fig. 5: DSC thermogram of the PMMA-MEK.3 organogel. Baseline shift corresponds to glass transition.

## Real inked paper sample

The applicative tests with the PMMA-MEK.3 organogel were carried out on a 19<sup>th</sup> century printed missal book (*“In officio et Missa solemni pro defunctis”*, 1852 AD) coming from a Florentine Church archive. The book shows numerous wax spots (see Fig. 6) all over the surface of the paper sheets, probably due to dropping of wax from candles used as a light source during reading sessions.

In order to characterize the wax contaminant, some of the spots from different areas shown in Fig. 6 were sampled. The wax samples were analyzed by ATR-FTIR (results not shown here), which indicated perfect overlap with the spectrum of paraffin wax, as highlighted by the presence of bands at  $2915$  and  $2848\text{ cm}^{-1}$  (CH stretching),  $1473\text{ cm}^{-1}$  (CH bending),  $1380\text{ cm}^{-1}$  ( $\text{CH}_3$  bending),  $728$  and  $719\text{ cm}^{-1}$  ( $\text{CH}_2$  rocking) [24–26].

## Application of the organogel

Both the PMMA-MEK.3 organogel and the PMMA-MEK gel previously developed were applied on the inked paper for the removal of paraffin wax (see Fig. 7). The cleaning tests were performed using flat gel sheets (ca.  $1.5 \times 1.5\text{ cm}^2$ , 2 mm thick), which were deemed easier to handle than the cylinder-shape gels for this specific



Fig. 6: Digital image of a 19<sup>th</sup> century missal, showing wax spots that jeopardize the inked paper sheets.

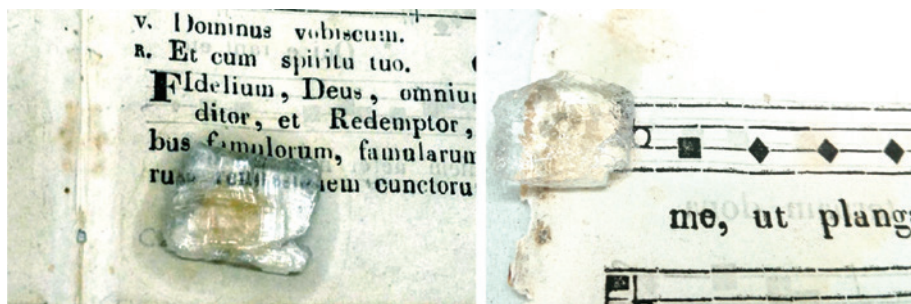


**Fig. 7:** (Right) Application of the PMMA-MEK organogel previously developed for the cleaning of painted canvas. The gel lacks the needed retentiveness for application on inked paper, as highlighted by the spreading of MEK across the paper surface. (Left) Application of the new PMMA-MEK.3 gel on the same paper document. The increased retentiveness of the new formulation avoids the uncontrolled spreading of MEK across the surface.



**Fig. 8:** (a1–2) Application of the PMMA-MEK organogel previously developed for the cleaning of painted canvas. (a1) Wax spot before cleaning. (a2) After the application and removal of the less retentive gel, a tideline has formed owing to the uncontrolled spreading of the solvent, which migrated carrying dissolved wax. (b1–3) Application of the new PMMA-MEK.3 gel. (b1) Wax spot before cleaning. (b2) The same area after the application of the gel. No tideline is observable, thanks to the improved retentiveness of the gel as compared to the previous formulation. (b3) Detail of the cleaning intervention showing the presence of wax before the removal (left) and the inked paper after removal of wax using the PMMA-MEK.3 organogel (right).

application. Figure 7 shows that the PMMA-MEK.3 has enough retentiveness to avoid the uncontrolled spreading of MEK across the paper surface, which instead occurs when the previous PMMA-MEK system is applied. A significant consequence is that the less controlled solvent release of the previous PMMA-MEK gel leads to the formation of tidelines (see Fig. 8a1–2). The latter form because the faster and less controlled release of solvent results in the solubilization of wax, which is transported by MEK as the solvent spreads through the paper fiber network. When the solvent finally evaporates, the dissolved material re-deposits forming the tideline. This is not observed when the PMMA-MEK.3 formulation is applied (see Fig. 8b1–2), owing to the increased retentiveness of the new gel, which avoids uncontrolled spreading of the solvent.

The better performance of the new systems is in agreement with the results of the physico-chemical characterization shown in the previous sections, which highlighted a slower solvent release, a lower solvent content, and a decreased mesoporosity of the new formulation as compared to the previous one. This result confirms that the gel synthetic procedure can be effectively tuned to improve the retentiveness of the PMMA network, which allows extending the use of the same class of gels to several cellulose-based substrates with different properties in terms of porosity, hydrophilicity, surface roughness, etc.

The most effective cleaning procedure consisted in applying the PMMA-MEK.3 gel directly on wax spots in two successive applications, each of about 15 min (total application time of 30 min), in order to obtain a gradual and controlled removal of the wax layer. After each application, the wax became swollen and softened, and partially adhered to the gel, detaching from the paper surface. After the second application, the swollen wax residues on paper were removed with gentle mechanical action using a dry cotton swab. Figure 8b3 shows the detail of the waxy area before and after cleaning with the PMMA-MEK.3 organogel. After the treatment, the white/yellow wax patina is consistently removed, and the ink is well readable.

Optical microscope analysis on the same spot showed the disappearance of the matte waxy layer after the cleaning intervention, to reveal the original paper fibers (see Fig. 9).

The efficiency of the treatment was checked using ATR-FTIR on the cleaning area.

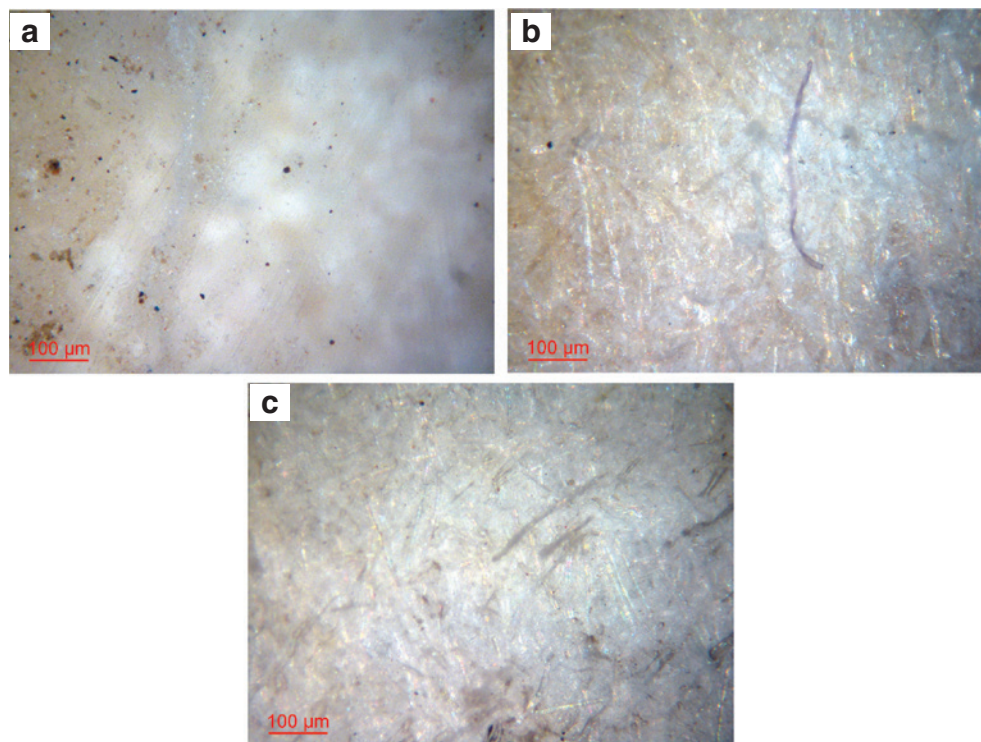


**Fig. 9:** Optical microscope images of the paper surface of the 19<sup>th</sup> century missal: (a) spot contaminated by paraffin wax; (b) the same spot after removal of the wax using the new PMMA-MEK.3 organogel; (c) a spot that was not contaminated with wax.

The spectrum of treated area (see Fig. 10) confirms the removal of paraffin wax, whose bands are almost no longer observable. Moreover, the most intense bands of PMMA at  $1726\text{ cm}^{-1}$  (C=O stretching) and  $1150\text{ cm}^{-1}$  ( $\nu_a$  C–O–C) are not observable in the spectrum of the cleaned paper surface (see Fig. 11), confirming the absence of gel residues as detectable by ATR-FTIR. In fact, the spectrum of the cleaned area overlaps with that of spots that were not contaminated by wax.

## Conclusions

In this work we synthesized a new organogel, based on MMA and MEK, specifically designed for the selective removal of aged wax layers from the surface of ancient (solvent-sensitive) inked paper. The new gel formulation was designed in order to improve on previous PMMA-based gels developed for the cleaning of canvas paintings, which lacked the desired retentiveness for extending their application also to paper substrates. To achieve this improvement, we systematically tuned the amount of cross-linker and monomer-solvent phase ratio used during the free radical polymerization of MMA in the MEK liquid phase, which allowed obtaining organogels with optimal characteristics in terms of retentiveness and mechanical properties (i.e. feasible handling and removal from the treated surface). The increased amount of cross-linker and the different solvent-monomer ratio used in the radical process, resulted in a decreased solvent content and mesoporosity of the gel network. In turn, this led to a slower and more gradual solvent release, both on porous and non-porous surfaces, as compared to the previous formulation.

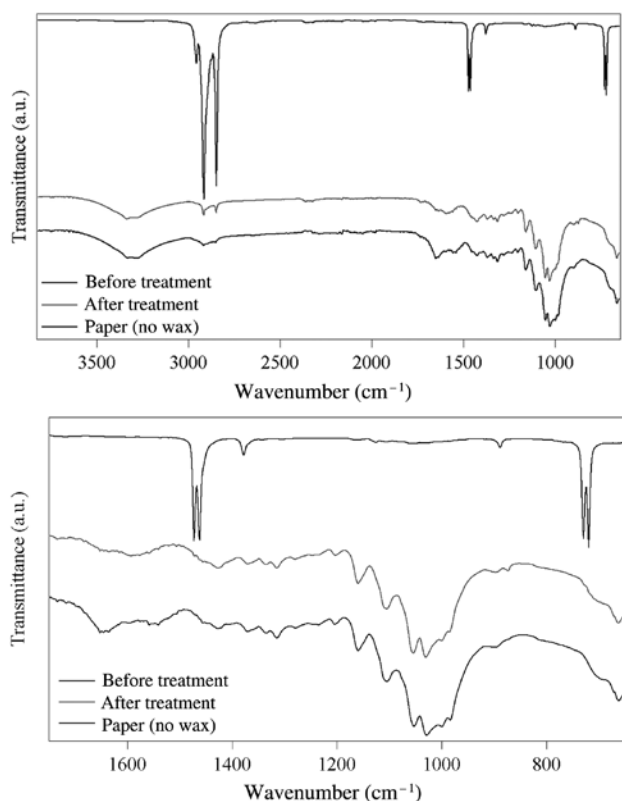


**Fig. 10:** ATR-FTIR spectra of the 19<sup>th</sup> century missal, showing the comparison between the spectra of paper before cleaning, paper after wax removal with the PMMA-MEK.3 gel, and paper that did not show any wax contamination. The bottom panel shows the 1600–650  $\text{cm}^{-1}$  region, to highlight that the bands of paraffin wax are almost not observable in the spectra of paper cleaned with the gel.

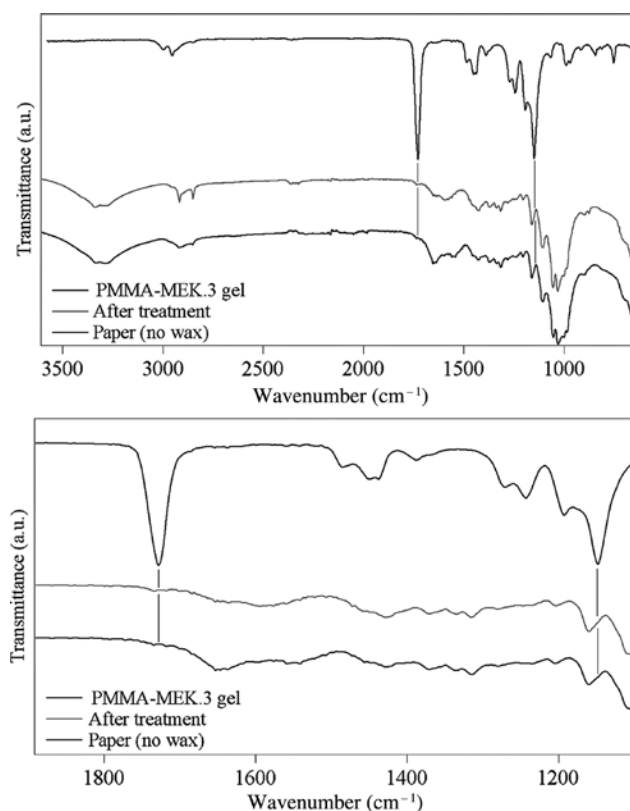


**Fig. 11:** Comparison between the ATR-FTIR spectra of paper after wax removal with the PMMA-MEK.3 gel, of paper that did not show wax contamination, and of the PMMA-MEK.3 gel. The bottom panel shows the 1800–1100  $\text{cm}^{-1}$  region, to highlight that the bands of the gel are not observable in the spectrum of the paper cleaned with the gel.

The PMMA-MEK organogels were applied on a 19<sup>th</sup> century inked document to remove spots of paraffin wax that hindered the readability and aesthetic appearance of the artifact. The performance of the new systems was compared to that of the previous formulation. The gel formulation previously developed (which worked well on varnished canvas paintings) led to uncontrolled spreading of MEK and to the formation of tidelines on the paper surface. On the other hand, the new PMMA-MEK system allowed a safer and more gradual release of solvent on the paper surface, which led to the gradual swelling and detachment of the wax contaminant. After the cleaning intervention, the gel can be removed without leaving polymer residues on the surface as verified by ATR-FTIR. Overall, this work validated the tunable synthesis of PMMA-based organogels as a process to produce versatile cleaning tools that can be used on different artistic surfaces, decreasing the risks of altering the original properties of the artifacts.

**Acknowledgments:** CSGI and European Union (project NANORESTART, H2020-NMP-21-2014/646063) are acknowledged for financial support. The authors acknowledge Maria Chiara Sbolci (University of Florence) for her cooperation during the tests on the 19<sup>th</sup> century missal. Ministero dell’Istruzione, dell’Università e della Ricerca, (Grant/Award Number: 646063) Horizon 2020.

## References

- [1] C. J. Shahani, G. Harrison. in *Works of Art on Paper: Books, Documents and Photographs*, V. Daniels, A. Donnithorne, P. Smith (Eds.), pp. 189–192, International Institute for Conservation of Historic and Artistic Works, London (2002).
- [2] A. Casoli, Z. Di Diego, C. Isca. *Environ. Sci. Pollut. Res.* **21**, 13252 (2014).

- [3] P. Baglioni, D. Chelazzi, R. Giorgi, G. Poggi. *Langmuir* **29**, 5110 (2013).
- [4] J. Domingues, N. Bonelli, R. Giorgi, P. Baglioni. *Appl. Phys. A* **114**, 705 (2014).
- [5] P. Baglioni, D. Chelazzi, R. Giorgi. *Nanotechnologies in the Conservation of Cultural Heritage – A compendium of materials and techniques*, pp. 98–99, Springer, Dordrecht (2015).
- [6] P. Baglioni, E. Carretti, D. Chelazzi. *Nat. Nanotechnol.* **10**, 287 (2015).
- [7] M. Baglioni, A. Bartoletti, L. Bozec, D. Chelazzi, R. Giorgi, M. Odlyha, D. Pianorsi, G. Poggi, P. Baglioni. *Appl. Phys. A* **114**, 122 (2016).
- [8] P. Baglioni, N. Bonelli, D. Chelazzi, A. Chevalier, L. Dei, J. Domingues, E. Fratini, R. Giorgi, M. Martin. *Appl. Phys. A* **121**, 857 (2015).
- [9] A.S. Mujumdar, S. Devahastin. *Fundamental principles of drying*, pp. 1–22, Exergex, Brossard, Canada (2000).
- [10] N. A. Peppas, R. W. Kormsmeier. *Hydrogels in Medicine and Pharmacy*, vol. 3, pp. 109–136, CRC Press, Boca Raton (1986).
- [11] P. Debye, A. M. Bueche. *J. Appl. Phys.* **20**, 518 (1949).
- [12] T. Canal, N. A. Peppas. *J. Biomed. Mater. Res. A* **23**, 1183 (1989).
- [13] F. Ikkai, M. Shibayama. *J. Polym. Sci. Part B.* **43**, 617 (2005).
- [14] S. Panyukov, Y. Rabin. *Phys. Rep.* **269**, 1 (1996).
- [15] L. Benguigui, F. Boue. *Eur. Phys. J. B.* **11**, 439 (1999).
- [16] B. V. Lebedev, I. B. Rabinovich. *Tr. Khim. Khim. Tekhnol.* **1**, 8 (1971).
- [17] L. I. Pavlinov, I. B. Rabinovich, N. A. Okladnov, S. A. Arzhakov. *Polymer. Sci. A* **9**, 539 (1967).
- [18] J. Biroš, T. Larina, J. Trekoval, J. Pouchly. *Colloid. Polym. Sci.* **260**, 27 (1982).
- [19] H. Teng, K. Koike, D. Zhou, Z. Satoh, Y. Koike, Y. Okamoto. *J. Polym. Sci. A* **47**, 315 (2009).
- [20] T. Ramanathan, S. Stankovich, D. A. Dikin, H. Liu, H. Shen, S. T. Nguyen, L. C. Brinson. *J. Polym. Sci.* **B45**, 2097 (2007).
- [21] M. E. Achour, A. Droussi, D. Medine, A. Oueriagli, A. Outzourhit, A. Belhadj Mohamed, H. Zangar. *Int. J. Phys. Sci.* **6**, 5075 (2011).
- [22] J. M. Hwu, G. J. Jiang, Z. M. Gao, W. Xie, W. P. Pan. *J. Appl. Polym. Sci.* **83**, 1702 (2002).
- [23] P. Thomas, R. S. Ernest Ravindran, K. B. R. Varma. *J. Therm. Anal. Calorim.* **115**, 1311 (2014).
- [24] C. J. Pouchert. *The Aldrich library of infrared spectra*, 2<sup>nd</sup> ed., Aldrich Chemical, Milwaukee, Wisconsin (1997).
- [25] F. J. Ludwig. *Anal. Chem.* **37**, 1737 (1965).
- [26] C. W. Meuse, P. E. Barker. *Appl. Immunohistochem. Mol. Morphol.* **17**, 547 (2009).